

Vector vortex beams generated by q-plates as a versatile route to direct fs laser surface structuring

Jijil JJ Nivas^{1,2}, Elaheh Allahyari^{1,2}, Filippo Cardano¹, Andrea Rubano¹, Rosalba Fittipaldi³, Antonio Vecchione³, Domenico Paparo⁴, Lorenzo Marrucci^{1,4}, Riccardo Bruzzese^{1,2}, Salvatore. Amoruso^{1,2,*}

¹*Dipartimento di Fisica “Ettore Pancini”, Università di Napoli Federico II, Complesso Universitario di Monte S. Angelo, Via Cintia, I-80126 Napoli, Italy,*

²*CNR-SPIN UOS Napoli, Complesso Universitario di Monte S. Angelo, Via Cintia, I-80126 Napoli, Italy*

³*CNR-SPIN, UOS Salerno, Via Giovanni Paolo II 132, I-84084 Fisciano, Italy*

⁴*National Research Council, Institute of Applied Science & Intelligent Systems (ISASI) ‘E. Caianiello’, Via Campi Flegrei 34, 80078 Pozzuoli (NA), Italy*

* Corresponding author: salvatore.amoruso@unina.it

Abstract

We report an experimental investigation on direct laser surface structuring with femtosecond vector vortex beams generated by means of q-plates with topological charges $q = 1, 3/2, 2, 5/2$. Structured light beams with spatially variant state of polarization and intensity are generated and applied to multi-pulse irradiation of a solid crystalline silicon target. The creation of a variety of surface structures, like laser induced periodic surface structures, multi-spot arrays and shaped ablation craters, is demonstrated by direct laser surface structuring with vector vortex beams at different values of q . The features of the surface structures are compared with the vector vortex beam characteristics at the focal plane, evidencing their relationship with the polarization and intensity profile of the laser beams. Our experimental findings show that vector vortex beams produced by q-plates can offer a valuable and versatile route to imprint unconventional surface structures on a solid target through a mask-free ablative process and step scan processing.

Keywords: Direct fs laser surface structuring; Vector Vortex Beams; Laser fabrication methods.

Highlights

- The fabrication of spatially variant LIPSS with Vector Vortex Beams is demonstrated.
- The realization of ablation craters with peculiar shapes is reported.
- The possibility to elaborate a variety of surface patterns is shown.

1. Introduction

Direct femtosecond laser processing is continuously showing significant achievements in the generation of surface structures [1–3]. The most intriguing example is the formation of self-organized quasi-periodic surface patterns, generally indicated as laser-induced periodic surface structures (LIPSS) [1]. Laser beam shaping is another valuable approach pursued to achieve mask-free surface and volume structuring [2,4].

In the last decades, the number of research fields trying benefits from the application of structured light beams with tailored intensity, polarization or phase is continuously increasing (e.g., microscopy, quantum optics and information, photonics, optical trapping, data communication, etc.) [5,6]. Recently, the use of structured light beams is also emerging in direct laser processing and surface structuring thanks to the development of efficient beam converters generating powerful pulses of complex light [7,8]. For example, fs structured light beams have been used to realize nano-cavities in glasses [9], nano-cones on silicon [10], micro-tubes in polymers [11], micro-disks on graphene sheets [12], etc. In this context, the direct link of the LIPSS orientation to the state of polarization (SoP) of the incident laser beam has led to the formation of peculiar quasi-periodic surface patterns by means of fs beams with spatially variant polarization and intensity distributions [13–17]. At the same time, surface structures have also been considered as a way to gain information of the characteristics of intense, structured light fields [8,18–21]. In most cases, structured laser beams with a cylindrically symmetric SoP (e.g. radial, azimuthal, spiral) and intensity profiles [13,15,16,18–20] are used, while other vector vortex (VV) light fields with more complex distributions of polarization and intensity are still rarely investigated [14,17,22].

Here we report on our ongoing research on direct femtosecond laser surface structuring with VV beams generated by q-plates. A q-plate is an optical device formed by a thin layer of liquid crystals. It essentially works as a spatially variant birefringent linear retarder with a singular pattern of the local optic axes, with a topological charge q , that allows the creation of light beams characterized by phase or polarization singularities [23–25]. Some interesting features of direct fs laser surface structuring of silicon with structured light beams generated by a q-plate were illustrated in previous studies [14,15,22]. Here, we further assess and extend the possibilities offered by complex light exploring various surface structures generated by using q-plates with a higher topological charge (namely, $q=1, 3/2, 2, 5/2$) and appropriate strategies to imprint multiple spots and create arrays of shaped structures. The produced surface structures are compared with the features of the VV beams at the focal plane. The various beams generated by the q-plates have been used to irradiate a crystalline silicon target with the aim of evidencing the versatility of this method in direct laser surface processing. The paper is organized as follows: Section 2 briefly reports the characteristics of the experimental setup. In section 3.1 we illustrate with some examples the spatially-variant LIPSS and the kind of shapes that can be produced by VV beams generated by a q-plate. Then, in Sect. 3.2 we address the imprinting of multiple spots in static irradiation achieved by means of a linear polarizer selecting a fraction of the beam. Finally, in Sect. 3.3 we discuss the fabrication of arrays of surface structures by a step scan approach.

2. Experimental.

Laser pulses of ≈ 35 fs duration at a wavelength of 800 nm are provided by a Ti:Sa laser system. The laser beam is characterized by a Gaussian spatial profile and linear polarization. Optical VV beams are generated by means of q-plates and focused, at normal incidence, onto the surface of a crystalline silicon target (intrinsic, (100)) by a plano-convex lens with a focal length of 75 mm. An electromechanical shutter selects the number of laser pulses, N , irradiating the surface of the target, which is mounted on a computer-controlled 3-axis translation stage. The surface structures generated in various experimental conditions are eventually characterized by a field-emission scanning electron microscope (FESEM).

3. Results and discussion.

A detailed analysis of the various beams that can be generated by the q-plates used in the present investigation ($q = 1, 3/2, 2, 5/2$) has been reported earlier [22]. A variety of VV beams can be achieved by controlling the birefringence optical retardation δ of the q-plate [24], that in our case is achieved by varying the peak-to-peak intensity of a square-wave voltage at 11 kHz delivered by a signal generator. Various examples of the VV beams used in the present investigation are illustrated in the following section.

3.1 VV beams generated by q-plates with $q = 1, 3/2, 2, 5/2$.

At a half-wave optical retardation $\delta = \pi$ (typically indicated as tuned case), the q-plate generates VV beams with an annular spatial profile. Panels (a) and (d) of Fig. 1 report simulated spatial maps of normalized intensity and SoP for two VV beams generated by exploiting tuned q-plates with topological charges of $q=1$ and $q=2$, respectively. The size of the annular VV beams depends on q , increasing at higher values of q [21]. The SoP of the VV beam can be rather complex, as for example shown Figs. 1(a) and (d), depending on the polarization direction of the input beam and the q-plate topological charge.

Panels (b-c) and (e-f) of Fig. 1 report the SEM images of the target surface, registered at different magnifications, after irradiation by the VV beams depicted in panels (a) and (d), respectively. The surface structures form after an irradiation sequence of N pulses at an energy E_0 that are $\{N = 200; E_0 = 30 \mu\text{J}\}$ for panel (b-c) and $\{N=100; E_0=80 \mu\text{J}\}$ for panel (e-f). The corresponding peak fluence values are $\approx 0.3 \text{ J/cm}^2$ for $q=1$ and $\approx 0.5 \text{ J/cm}^2$ for $q=2$ [21]. In both cases, one can clearly observe the formation of the typical low spatial frequency LIPSS (LSFL) produced in surface structuring of silicon (i.e. ripples and grooves [1,26]) with a spatially variant orientation that depend on the SoP of the VV beam. In particular, a shallow crater is imprinted on the silicon target surface with supra-wavelength grooves (parallel to the local VV beam polarization) located in a central annular area, at larger fluence, surrounded by sub-wavelength ripples (normal to the local VV beam polarization). The clean edge of the craters indicates that our experimental conditions correspond to the regime of soft ablation occurring close to threshold for material removal and affecting only the very surface layers of materials (typical depth of the order of 100 nm) for which the induced morphological changes are typically referred as surface structures [1,3,27].

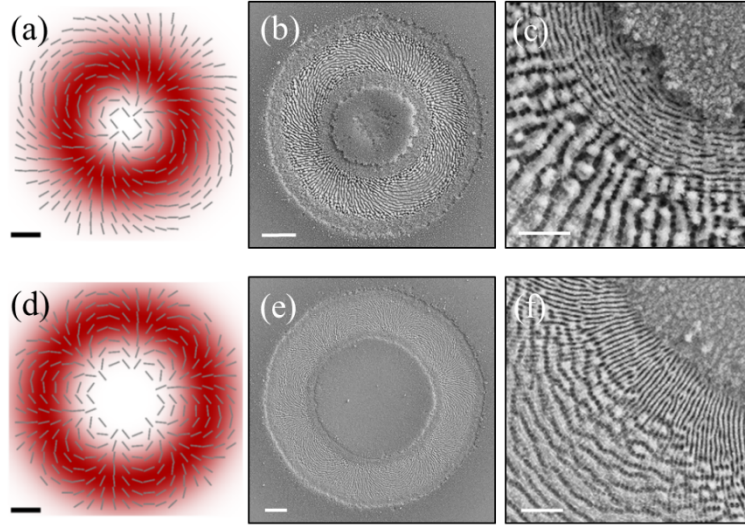


Fig. 1: Panels (a) and (d) report maps of the VV beam at the focal plane for $q=1$ and $q=2$, respectively, illustrating the annular profile of the intensity and the spatial distribution of the SoP. The intensity is normalized to its maximum value and the scale bar is 20 μm . Panels (b-c) and (e-f) show SEM images of the surface structures produced on the silicon target by the VV beams produced by q -plates with topological charge $q=1$ and $q=2$, respectively, registered at different magnification. The scale bars are 20 μm in (b) and (e) and 5 μm in (c) and (f).

Recently, we addressed the possibility of generating unconventional shapes by tailoring the laser intensity profiles by exploiting the tuning of the q -plate optical retardation δ [22]. This method offers a way to vary the intensity distribution of the VV beam by generating an optical field given by a superimposition of the unconverted part of the input Gaussian field with an annular VV beam generated in tuned conditions, whose proportion depend on the value of δ [22]. As an example of the VV beams generated in this way, the lower panels of Fig. 2(a) report simulated spatial maps of the fluence at the focal plane for a q -plate with $q=1$ for three different values of the optical retardation δ . Moreover, contour lines corresponding to a local fluence value of 0.1 J/cm² are reported on the fluence maps as dashed curves. One can observe fluence spatial profiles resembling bowtie (see, e.g., $\delta=0.7\pi$ and 1.5π) or donut-like shapes (e.g. $\delta=0.9\pi$). The upper panels of Fig. 2(a) report the shapes generated on the target surface by a sequence of $N=100$ laser pulses at an energy $E_0=20$ μJ . The corresponding experimental values of the optical retardation δ approximate the value of the corresponding map (lower panels) within an accuracy of $\pm 5\%$. The shapes of the craters present general features in fairly good agreement with the fluence maps, within the limited statistics and the uncertainties of experimental parameters like laser pulse energy and spot size as well as pulse-to-pulse fluctuations. Interestingly, this comparison displays a proof-of-principle approach to elaborate unusual craters' shapes that can be employed to generate peculiar surface structures that might be of interest in mask-free subtractive manufacturing through localized ablation or in material transfer methods, like direct write or laser-induced forward transfer techniques.

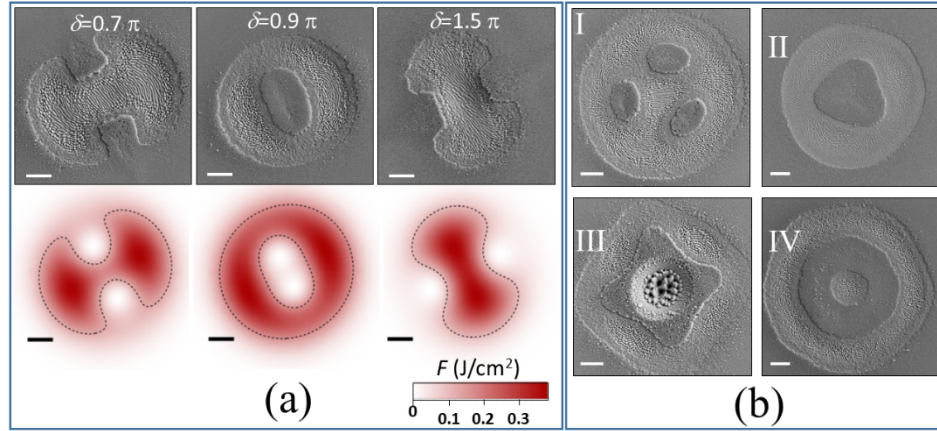


Fig. 2: (a) Upper panels: examples of shapes imprinted on the target surface after irradiation with a sequence of $N=100$ laser pulses at an energy $E_0=20 \mu\text{J}$ with VV beams generated by a q-plate with $q=1$ for various values of the optical retardation δ . Lower panels: maps of the VV beam fluence spatial profile for corresponding values of δ ; the fluence variation is shown according to the false color scale reported on the right. (b) Examples of shapes generated by other VV beams: (I) $q=3/2$, $N=200$, $E_0=65 \mu\text{J}$; (II) $q=3/2$, $N=50$, $E_0=100 \mu\text{J}$; (III) $q=2$, $N=200$, $E_0=65 \mu\text{J}$; (IV) $q=5/2$, $N=50$, $E_0=100 \mu\text{J}$. The scale bar in each panel is 20 μm .

Fig. 2(b) reports SEM images of some exemplificative crater shapes that can be generated by VV beams with higher values of the q-plate topological charge q . For $q=3/2$, panel (I) shows the formation of three isolated islands, while panel (II) reports a central region with a blunt triangular shape of non-ablated material within the crater. For $q=2$, panel (III) shows a shape resembling a 4-pointed star with a central hole, while for $q=5/2$ panel (IV) shows a ring of non-ablated material in the crater center. These are few of the various shapes that can be achieved by optical retardation tuning of the q-plates [22].

3.2 Multi-spot patterns.

Here we illustrate an optical shaping of the VV beam intensity producing multiple beam spots at the focal plane. This kind of structured beams can be of interest in various applications like multi-pixels transfer of material in direct write laser techniques, mask-free subtractive printing through localized ablation, etc. [2,4,28]. This is achieved by filtering the VV beam in tuned conditions with a linear polarizer, thus obtaining a multi-spot pattern in the focal plane with $4q$ intense lobes. Fig. 3(a) shows an example of the 4 lobes intensity pattern for $q=1$ for the case of Fig. 1(a) after filtering with a linear polarizer transmitting only the parts of the beam that are horizontally polarized. The corresponding SEM image of the sample surface obtained for an irradiation sequence of $N=50$ pulses at an energy $E_0=40 \mu\text{J}$ is reported in Fig. 3(b), which clearly shows the formation of a tetrameric ablative micro-pattern. Panels (c) and (d) of Fig. 3 report two further examples obtained by exploiting the VV beams generated by q-plates with $q=2$ and $q=5/2$, respectively, that after filtering with a vertically transmitting linear polarizer imprint a pattern composed of 8 and 10 lobes on the target surface. Hence, this demonstrates that a variety of patterns with a number of lobes $n = 4q$ can be generated by polarization filtering of VV beams generated by q-plates with a topological charge q in tuned conditions.

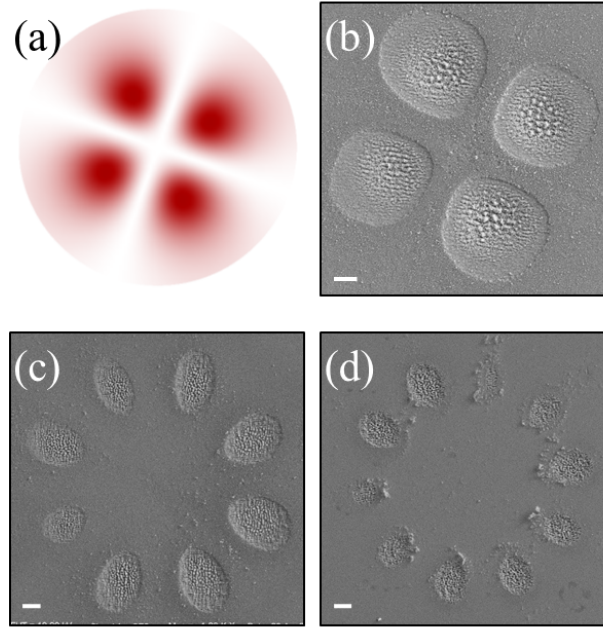


Fig. 3: Panel (a) reports an example of intensity map of the VV beam for $q=1$ after filtering with a linear polarizer transmitting the horizontal polarization, which illustrates the formation of a multi-spot pattern at the focal plane. Panel (b) shows a SEM image of the surface pattern produced by the beam reported in (a), for $N=50$ and $E_0=40 \mu\text{J}$. Panels (c) and (d) report SEM images of surface patterns produced by VV beams filtered by a vertically transmitting linear polarizer for $q=2$ ($N=100$ and $E_0=70 \mu\text{J}$) and $q=5/2$ ($N=200$ and $E_0=50 \mu\text{J}$). The scale bars in panels (b), (c) and (d) are $20 \mu\text{m}$.

3.3 Patterns fabrication by step scanning approach.

Here we illustrate the possibility of fabricating arrays of surface structures with peculiar shapes as those obtained by fluence spatial profile tuning through a step scanning approach. In this way, direct surface writing of a large area can be achieved with a repetition of an elemental crater shape and its surface structures in a given spatial arrangement. Such an approach has been recently applied to elaborate large area of biomimetic surfaces composed of hierarchical structures on Ni showing super-hydrophobic behaviour by using a phase plate capable of producing radially and azimuthally polarized VV beams [13]. In the following, we show some examples of patterns obtained by step scan with VV beams produced by a q-plate with topological charge $q=1$. The used number of pulses for each elemental crater is $N=100$ and the pulse energy is $E_0=20 \mu\text{J}$.

Fig. 4 reports SEM images of patterns fabricated by using a VV beam generated in tuned conditions ($\delta=\pi$). Three examples are reported illustrating how the morphological features of the surface varies as a function of the step size Δ . Panels (b), (d) and (f) report zoomed views registered at higher magnification of the corresponding SEM images (a), (c) and (e). The insets in dashed boxes are SEM images illustrating the fine texture of the surface decorated with LIPSS and separating the written structures. From these images, one can observe that the LIPSS namely form in the annular region irradiated by the intense part the VV beam, while the surviving areas of the

pristine sample surface are mainly decorated with nanoparticles. The diameter of the elemental crater is $D \approx 110 \mu\text{m}$. It is worth noticing the rather good reproducibility of the craters produced in each step of the writing process.

At $\Delta = 120 \mu\text{m}$, the SEM images reported in panels (a) and (b) of Fig. 4, show an array of well separated annular craters (as indicated by the dashed yellow lines in panel (b)) inscribed within a connected background of the pristine sample surface. Reducing Δ to values smaller than D the craters partially overlap, as for example shown in panels (c) and (d) for $\Delta = 100 \mu\text{m}$. This leads to a surface morphology composed by a periodic array of disks with a diameter of $\approx 45 \mu\text{m}$ (upper dashed yellow line in panel (d)), corresponding to the central non-ablated area of each crater, intercalated with a secondary pattern of inclined squares with a side of $\approx 30 \mu\text{m}$ (lower dashed yellow line in panel (d)). Finally, at still lower value of Δ , e.g. for $\Delta = 80 \mu\text{m}$ as reported in panels (e) and (f), a regular array of disks separated by a background fully decorated with LIPSS is eventually produced.

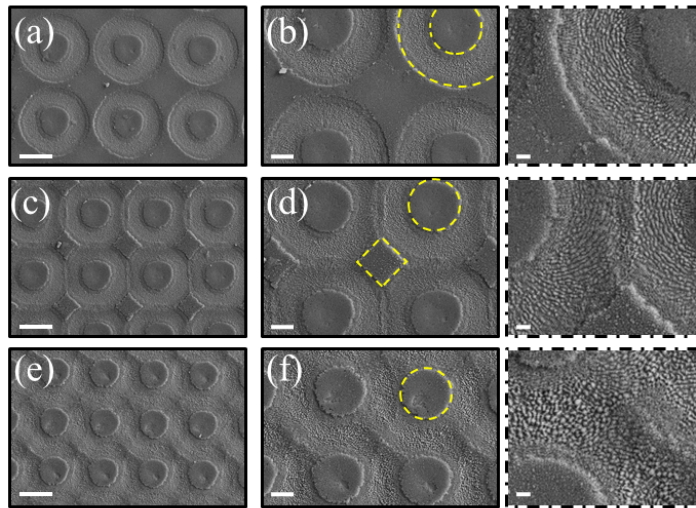


Fig. 4: SEM images of the patterns obtained by using a VV beam generated by a q-plate with topological charge $q=1$ in tuned conditions. The number of pulses for each elemental crater is $N=100$ and the pulse energy is $E_{\sigma}=20 \mu\text{J}$. The nominal step size of the translation stage is $\Delta=120 \mu\text{m}$ for (a) and (b), $\Delta=100 \mu\text{m}$ for (c) and (d), $\Delta=80 \mu\text{m}$ for (e) and (f). Panels (b), (d) and (f) are zoomed views of panels (a), (c) and (e), respectively. The scale bars are: $50 \mu\text{m}$ for panels (a), (c) and (e); $20 \mu\text{m}$ for panels (b), (d) and (f). The dashed yellow lines in panels (b), (d) and (f) indicate the central non-ablated area of each crater. The insets in dashed boxes on the right show zoomed views of the corresponding left panels illustrating the fine texture of the surface separating the written structures and decorated with LIPSS. The scale bar in the insets is $5 \mu\text{m}$.

We turn now to illustrate in Fig. 5 the case of patterns fabricated by repeating shaped craters produced by a VV beam in un-tuned conditions. As an example, we selected the case of a bow-tie shape occurring for $\delta \approx 0.7\pi$. Three examples are reported illustrating various arrangements of the periodic arrays and the fairly good reproducibility of the craters. Panels (b), (d) and (f) report zoomed views registered at higher magnification of the corresponding SEM images (a), (c) and (e). Panel (a) of Fig. 5 reports a pattern of bow-tie shaped craters with one of the main symmetry axis aligned along the horizontal position. The centers of two consecutive

craters are separated by 120 μm along both the horizontal and vertical directions. The distance between the closest edges of two consecutive craters is $\approx 20 \mu\text{m}$ along the horizontal and $\approx 45 \mu\text{m}$ along the vertical directions, respectively.

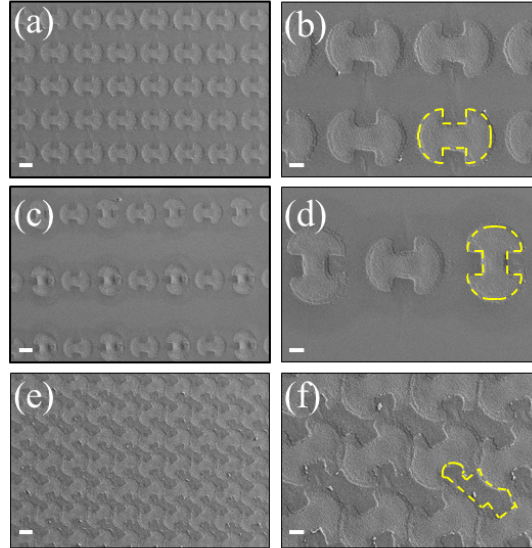


Fig. 5: SEM images of the patterns obtained by using a VV beam generated by a q-plate with topological charge $q=1$ in un-tuned conditions ($\delta=0.7\pi$). The number of pulses for each elemental crater is $N=100$ and the pulse energy is $E_0=20 \mu\text{J}$. Each right panel is a zoomed view of the corresponding left one. The scale bars are: 50 μm for panels (a), (c) and (e); 20 μm for panels (b), (d) and (f). The unitary tiles of the pattern are evidenced by dashed yellow lines in the left panels.

The orientation of the crater shape can be varied by acting on the direction of the input laser linear polarization to the q-plate, as shown for example in panels (c) and (d) where two consecutive elemental tiles of the array are rotated by 90° at each scanning step. In the case displayed in Figs. 5 (a) and (b), the centers of two consecutive craters are separated by 120 μm along the horizontal and 360 μm along vertical, but other distances and arrangements can be easily obtained. This feature of the laser writing process can effectively allow elaborating complex periodic arrays in which the repetitive units are made of elementary tiles composed of various craters oriented in different directions or with diverse shapes, since both input polarization and optical retardation can be easily controlled by using a rotating half wave plate and the q-plate driving voltage, respectively. Moreover, by appropriately changing the step size during the scan also aperiodic surface patterns can be fabricated.

Finally, panels (e) and (f) of Fig. 5 illustrate an example of pattern that can be achieved by writing bow-tie shaped craters with their longer axis inclined at $\approx 30^\circ$ and a step size ($\approx 100 \mu\text{m}$) slightly smaller than their major axis length ($\approx 110 \mu\text{m}$). In such a case the repetitive unit of the regular array is formed by the non-ablated areas left among the various ablation craters produced during the step scan processing and can assume a rather peculiar shape as that shown for example in Fig. 5 (see the yellow line in panel (f), e.g.). The elementary tiles of the pattern will be separated by a background carpet of structured surface with LIPSS and nanostructures.

A variety of pattern can be possibly achieved by changing the step parameters and the shape and size of the elementary craters by voltage tuning and appropriate selection of the q-plate topological charge.

4. Conclusions

In summary, we have presented an experimental investigation illustrating the various possibilities offered by direct fs laser surface structuring with VV beams generated by q-plates. Firstly, we have illustrated the different possibilities offered by VV beams produced by q-plates with different topological charges (namely, $q=1, 3/2, 2$ and $5/2$). In particular, we have addressed both the formation of spatially-variant LIPSS for annular VV beams generated by q-plates in tuned conditions ($\delta=\pi$) and the imprinting of peculiar shapes through variation of the laser fluence spatial profile at the focal plane by tuning the value of the optical retardation δ . Then, we have considered a facile way of obtaining a multi-spot beam pattern in the focal plane by a polarization filtering of the VV beam through a linear polarizer. Finally, the elaboration of surface patterns was illustrated through a spot-by-spot step scan approach that allows covering large area of the target sample. This approach can allow producing a variety of surface patterns in form of periodic or aperiodic arrays of shaped non-ablated island decorated with nanoparticles separated by a carpet of LIPSS and surface structures. Although the fabrication of all these surface morphologies was demonstrated in the case of silicon, the method can be directly applied to other kind of target materials to elaborate peculiar surface structured on bulk targets but also realize patterned surfaces on thin films by subtractive manufacturing. Hence, our approach of direct laser surface structuring with VV beams with q-plated shows a great potential, easy and compact way to tailor the laser beam characteristics (e.g. polarization and intensity) providing access to a plethora of complex surface structures and patterns. The new concept in fs laser structuring of materials brought about by our investigations can be considered as an emerging step towards more versatile laser based fabrication technique. The full exploration of its potential deserve further work and development before it can be a competitive technology. However, it already shows interesting achievements and promise of future potential applications in elaborating complex surfaces and gain or improve their functionality.

Acknowledgements

J. JJ N., A.R., and R.B. acknowledge the partial support from the research project “FAVOLA” funded by Università degli Studi di Napoli “Federico II.” L.M., F.C., and A.R. acknowledge the partial support by the European Research Council (ERC), under Grant No. 694683 (PHOSPhOR).

References

- [1] J. Bonse, S. Höhm, S. V. Kirner, A. Rosenfeld, J. Krüger, Laser-induced periodic surface structures – a scientific evergreen, *IEEE J. Sel. Top. Quantum Electron.* 23 (2017) 9000615. doi:10.1109/jstqe.2016.2614183.
- [2] M. Malinauskas, A. Žukauskas, S. Hasegawa, Y. Hayasaki, V. Mizeikis, R. Buividas, S. Juodkazis, Ultrafast laser processing of materials: from science to industry, *Light Sci. Appl.* 5 (2016) e16133–e16133. doi:10.1038/lsa.2016.133.
- [3] A.Y. Vorobyev, C. Guo, Direct femtosecond laser surface nano/microstructuring and its applications, *Laser Photonics Rev.* 7 (2013) 385–407. doi:10.1002/lpor.201200017.
- [4] M. Duocastella, C.B. Arnold, Bessel and annular beams for materials processing, *Laser Photon. Rev.* 6 (2012) 607–621. doi:10.1002/lpor.201100031.
- [5] H. Rubinsztein-Dunlop, A. Forbes, M. V Berry, M.R. Dennis, D.L. Andrews, M. Mansuripur, C. Denz, C. Alpmann, P. Banzer, T. Bauer, E. Karimi, L. Marrucci, M. Padgett, M. Ritsch-Marte, N.M. Litchinitser, N.P. Bigelow, C. Rosales-Guzmán, A. Belmonte, J.P. Torres, T.W. Neely, M. Baker, R. Gordon, A.B. Stilgoe, J. Romero, A.G. White, R. Fickler, A.E. Willner, G. Xie, B. McMorran, A.M. Weiner, Roadmap on structured light, *J. Opt.* 19 (2017) 013001. doi:10.1088/2040-8978/19/1/013001.
- [6] J. Secor, R. Alfano, S. Ashrafi, *Complex Light*, IOP Publishing, 2016. doi:10.1088/978-0-7503-1371-1.
- [7] Q. Zhan, Cylindrical vector beams: from mathematical concepts to applications, *Adv. Opt. Photonics.* 1 (2009) 1. doi:10.1364/AOP.1.000001.
- [8] C. Hnatovsky, V. Shvedov, W. Krolikowski, A. Rode, Revealing Local Field Structure of Focused Ultrashort Pulses, *Phys. Rev. Lett.* 106 (2011) 123901. doi:10.1103/PhysRevLett.106.123901.
- [9] C. Hnatovsky, V.G. Shvedov, W. Krolikowski, A. V. Rode, Materials processing with a tightly focused femtosecond laser vortex pulse, *Opt. Lett.* 35 (2010) 3417. doi:10.1364/OL.35.003417.
- [10] M.G. Rahimian, F. Bouchard, H. Al-Khazraji, E. Karimi, P.B. Corkum, V.R. Bhardwaj, Polarization dependent nanostructuring of silicon with femtosecond vortex pulse, *APL Photonics.* 2 (2017) 086104. doi:10.1063/1.4999219.
- [11] L. Yang, D. Qian, C. Xin, Z. Hu, S. Ji, D. Wu, Y. Hu, J. Li, W. Huang, J. Chu, Direct laser writing of complex microtubes using femtosecond vortex beams, *Appl. Phys. Lett.* 110 (2017) 221103. doi:10.1063/1.4984744.
- [12] B. Wetzel, C. Xie, P.-A. Lacourt, J.M. Dudley, F. Courvoisier, Femtosecond laser fabrication of micro and nano-disks in single layer graphene using vortex Bessel beams, *Appl. Phys. Lett.* 103 (2013) 241111. doi:10.1063/1.4846415.
- [13] E. Skoulas, A. Manousaki, C. Fotakis, E. Stratakis, Biomimetic surface structuring using cylindrical vector femtosecond laser beams, *Sci. Rep.* 7 (2017) 45114. doi:10.1038/srep45114.
- [14] J.J. Nivas, F. Cardano, Z. Song, A. Rubano, R. Fittipaldi, A. Vecchione, D. Paparo, L. Marrucci, R. Bruzzese, S. Amoruso, Surface Structuring with Polarization-Singular Femtosecond Laser Beams Generated by a q-plate, *Sci. Rep.* 7 (2017) 42142. doi:10.1038/srep42142.
- [15] J. JJ Nivas, S. He, A. Rubano, A. Vecchione, D. Paparo, L. Marrucci, R. Bruzzese, S. Amoruso, Direct Femtosecond Laser Surface Structuring with Optical Vortex Beams Generated by a q-plate, *Sci. Rep.* 5 (2015) 17929. doi:10.1038/srep17929.
- [16] G.D. Tsididis, E. Skoulas, E. Stratakis, Ripple formation on nickel irradiated with radially polarized femtosecond beams, *Opt. Lett.* 40 (2015) 5172. doi:10.1364/OL.40.005172.
- [17] K. Lou, S.-X. Qian, X.-L. Wang, Y. Li, B. Gu, C. Tu, H.-T. Wang, Two-dimensional microstructures induced by femtosecond vector light fields on silicon, *Opt. Express.* 20 (2012) 120. doi:10.1364/OE.20.000120.
- [18] J. JJ Nivas, S. He, K.K. Anoop, A. Rubano, R. Fittipaldi, A. Vecchione, D. Paparo, L. Marrucci, R. Bruzzese, S. Amoruso, Laser ablation of silicon induced by a femtosecond optical vortex

- beam, *Opt. Lett.* 40 (2015) 4611. doi:10.1364/OL.40.004611.
- [19] Y. Jin, O.J. Allegre, W. Perrie, K. Abrams, J. Ouyang, E. Fearon, S.P. Edwardson, G. Dearden, Dynamic modulation of spatially structured polarization fields for real-time control of ultrafast laser-material interactions, *Opt. Express*. 21 (2013) 25333. doi:10.1364/OE.21.025333.
- [20] O.J. Allegre, Y. Jin, W. Perrie, J. Ouyang, E. Fearon, S.P. Edwardson, G. Dearden, Complete wavefront and polarization control for ultrashort-pulse laser microprocessing, *Opt. Express*. 21 (2013) 21198. doi:10.1364/OE.21.021198.
- [21] E. Allahyari, J. JJ Nivas, F. Cardano, R. Bruzzese, R. Fittipaldi, L. Marrucci, D. Paparo, A. Rubano, A. Vecchione, S. Amoruso, Simple method for the characterization of intense Laguerre-Gauss vector vortex beams, *Appl. Phys. Lett.* 112 (2018) 211103. doi:10.1063/1.5027661.
- [22] J. JJ Nivas, E. Allahyari, F. Cardano, A. Rubano, R. Fittipaldi, A. Vecchione, D. Paparo, L. Marrucci, R. Bruzzese, S. Amoruso, Surface structures with unconventional patterns and shapes generated by femtosecond structured light fields, *Sci. Rep.* 8 (2018) 13613. doi:10.1038/s41598-018-31768-w.
- [23] L. Marrucci, C. Manzo, D. Paparo, Optical Spin-to-Orbital Angular Momentum Conversion in Inhomogeneous Anisotropic Media, *Phys. Rev. Lett.* 96 (2006) 163905. doi:10.1103/PhysRevLett.96.163905.
- [24] L. Marrucci, E. Karimi, S. Slussarenko, B. Piccirillo, E. Santamato, E. Nagali, F. Sciarrino, Spin-to-orbital conversion of the angular momentum of light and its classical and quantum applications, *J. Opt.* 13 (2011) 064001. doi:10.1088/2040-8978/13/6/064001.
- [25] F. Cardano, E. Karimi, S. Slussarenko, L. Marrucci, C. de Lisio, E. Santamato, Polarization pattern of vector vortex beams generated by q-plates with different topological charges, *Appl. Opt.* 51 (2012) C1. doi:10.1364/AO.51.0000C1.
- [26] S. He, J.J. Nivas, A. Vecchione, M. Hu, S. Amoruso, On the generation of grooves on crystalline silicon irradiated by femtosecond laser pulses, *Opt. Express*. 24 (2016) 3238. doi:10.1364/OE.24.003238.
- [27] J. Bonse, S. Baudach, J. Krüger, W. Kautek, M. Lenzner, Femtosecond laser ablation of silicon-modification thresholds and morphology, *Appl. Phys. A Mater. Sci. Process.* 74 (2002) 19–25. doi:10.1007/s003390100893.
- [28] A.A. Kuchmizhak, A.P. Porfirev, S.A. Syubaev, P.A. Danilov, A.A. Ionin, O.B. Vitrik, Y.N. Kulchin, S.N. Khonina, S.I. Kudryashov, Multi-beam pulsed-laser patterning of plasmonic films using broadband diffractive optical elements, *Opt. Lett.* 42 (2017) 2838. doi:10.1364/OL.42.002838.